IEEE Access
Multidisciplinary | Rapid Review | Open Access Journal

Received August 7, 2020, accepted September 7, 2020, date of publication September 9, 2020,
date of current version September 22, 2020.

Digital Object Identifier 10.1109/ACCESS.2020.3022996

Dynamic Modeling of the Active Magnetic Bearing System Operating in Base Motion Condition

YUANPING XU, (Member, IEEE), QUAN SHEN, YUE ZHANG, JIN ZHOU, AND CHAOWU JIN
College of Mechanical and Electrical Engineering, Nanjing University of Aeronautics and Astronautics, Nanjing 210016, China

Corresponding author: Jin Zhou (zhj@nuaa.edu.cn)

This work was supported in part by the National Natural Science Foundation of China under Grant 51905263, in part by the Jiangsu Natural Science Youth Fund under Grant BK20190412, and in part by the Jiangsu Postdoctoral Research Funding under Grant 2019K188.

ABSTRACT Active magnetic bearing (AMB) has been increasingly applied in high-speed rotating machinery applications because of the inherent merit of providing contactless magnetic force to levitate rotor. Generally, rotor AMB systems are applied in the static base situation whereas the recent work has also demonstrated their applicability in moving base conditions. Compared with traditional static base condition, the base motion condition is more complicated for rotor AMB system. For a better controller design and dynamic analysis, the dynamic modeling of AMB system operating in base motion condition is critical. However, the dynamics modeling of AMB system working in base motion condition has been rarely reported. Particularly, the rotational base motions are always neglected. Herein, in this work, based on a double-gimbal system model, we propose and develop a dynamic modeling method for AMB system considering both translational and rotational base motions. The derivation reveals that the translational base motion is equivalent to the external force applied to the rotor and the rotational base motion is equivalent to the external torque applied to the rotor. Furthermore, making use of the proposed dynamic model, we also analyze the dynamics of rotor displacement in the impact base motion condition from the aspects of excitation amplitude, pulse width and supporting parameters.

INDEX TERMS Active magnetic bearing, modeling, base motion, dynamics.

I. INTRODUCTION

Active magnetic bearing (AMB) is an electromagnetic device that provides magnetic force to suspend shaft other than conventional bearings relying on mechanical forces [1]. With the inherent distinguished features including absence of mechanical wear, elimination of lubrication, long life expectation, tunable stiffness and damping, as well as high attainable rotating speeds, AMBs have been increasingly applied in compressors, bearingless motors and other high-speed rotating machinery applications [2]–[4].

Typically, most of the AMB systems are applied in the stationary applications. The recent advances in AMB systems has also permitted their capability in base motion conditions such as hybrid electric vehicles, submarine propulsion systems, jet engines and spacecraft control moment gyro [5]–[9]. In general, the AMB system is open loop unstable and consequently feedback control is critical for levitation. Compared with conventional static base condition, the base motion conditions are more complicated as aggregate vibration of internal rotor dynamic vibrations and external base vibrations are both required to be considered. Thus, it is challenging for the controller design of AMB system operating in base motion conditions.

For conventional rotor bearing system, the system dynamics under base motion condition has already trigged attention from both academia and industry [10]–[15]. However, to date, the research work regarding AMB controller design are mainly based on static base conditions and only a few has focused on controller design linked to base motion conditions. For instance, Kasarda *et al.* [16] modified the PID controller gains on a non-rotating test rig with a single magnetic bearing mounted on a shaker to detect the effect of sinusoidal base motion. Cole *et al.* [17] designed controllers that were capable of attenuating vibration arising from either directly applied to the rotor or transmitted through the bearings owing to base motion. Kang [18], Kang *et al.* [19] presented an optimal base acceleration feedforward controller

The associate editor coordinating the review of this manuscript and approving it for publication was Mark Kok Yew Ng.

using filtered-X least-mean-square (LMS) algorithm and sliding mode controller to reduce the base motion response. Sim *et al.* [20] modeled the base motion as the dynamic disturbances and designed controllers to compensate the disturbances. The experimental results indicated that the performance of the proposed controllers for the AMB system is satisfactory in compensating for the disturbances due to the base motion. Marx and Nataraj [21] developed a novel method which combined PD feedback with feedforward optimal control to suppress rotor motion caused by base excitation. Zhu [22] experimentally analyzed the dynamic behavior of AMB system with impact load and found that the PID controller has limited capability in suppressing the impact load. Zhang [23] developed a coupled dynamic model for rotor AMBs while only base translational motion is considered. Soni *et al.* [24] evaluated the parametric stability of active rotor AMB system with a novel control law subjected to periodic base motion. Additionally, attempts have been made in the maglev train system due to the similar dynamic equation as compared with AMB system. For instance, Han [25] established a dynamic modeling method of maglev train. Sun *et al.* [26], [27] proposed the adaptive sliding mode control and adaptive neural-fuzzy robust position control algorithm for maglev train disturbance suppression.

Despite the effort in controller design for AMB system operating in base motion condition, it should be noted that most of the proposed designs were based on experimental results. The dynamics modeling of AMB system working in base motion condition has been rarely reported and rotational base motions are always neglected. In this regard, it is essential to develop the dynamic modeling of AMB system operating in base motion condition for a better controller design and dynamic analysis.

Herein, in this work, we aim to fill this gap. For the first time, a dynamic modeling method for AMB system operating in base motion condition is developed and presented wherein both translational and rotational base motions are both considered. Additionally, making use of the proposed dynamic model, we also analyze the dynamics of rotor displacement in the impact base motion condition as impact base motion may cause serious damage to AMB system.

The remainder of the paper is organized as follows. Section 2 describes the AMB system adopted in this paper. Section 3 presents the modeling method of AMB system considering base motion. The effect of the impact base motion on the dynamics are presented in Section 4. Conclusions are drawn in Section 5.

II. DESCRIPTION OF THE AMB SYSTEM

In this work, the AMB system was designed and built as a home-made research platform, as shown in Fig. 1. The length of rotor is 336mm. Two radial and two thrust AMBs provide magnetic levitation force for the rotor. The decentralized PID control is employed to stabilize the rotor AMB system.

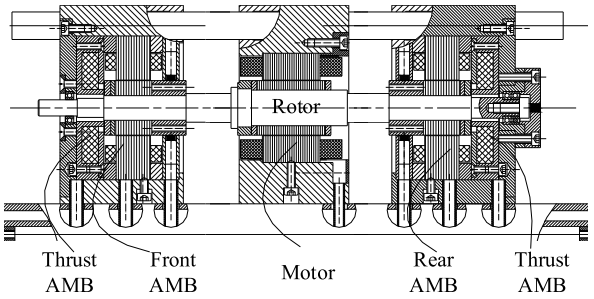

FIGURE 1. The schematic view of the rotor AMBs test rig.

TABLE 1. Parameters for the AMB.

Symbol	Parameter	Values
S	Air gap (AMB clearance)	0.3 mm
A	Polar face area	2.0×10^{-4} m^2
n_a	Windings of a coil	0 mm
β_a	Half angle between two poles	22.5 degree

Table 1 lists the radial AMB parameters employed in this system. Since the maximum speed of this test rig is far more behind the rotor first bending critical speed, the rigid rotor model is adopted in the following mathematic modeling derivation.

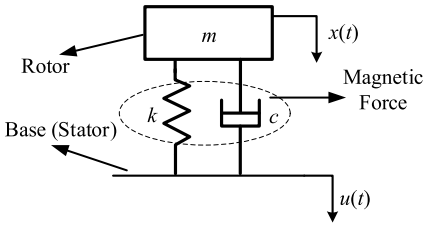

FIGURE 2. Rotor motion considering base motion in the vertical direction.

III. MODELING ROTOR AMB SYSTEM WITH BASE MOTION

A. MODELING THE TRANSLATIONAL BASE MOTION

Fig. 2 presents the rotor center of mass motion considering base motion in vertical direction, wherein x is rotor displacement, u is base motion displacement, m is the rotor mass, k is the stiffness and c is the damping provided by AMB. The system equation of motion can be written as,

$$m\ddot{x} + c\dot{x} + kx = c\dot{u} + ku \tag{1}$$

Given that the stator is fixed on the base, the sensor detects the relative displacement δ between the rotor and the base, which could be written as,

$$\delta(t) = x(t) - u(t) \tag{2}$$

Substitute Eq. (2) into Eq. (1) and obtain

$$m\ddot{\delta} + c\dot{\delta} + k\delta = -m\ddot{u} \tag{3}$$

Eq. (3) indicates that upon the translational base excitation, the motion of rotor relative to the base is equivalent to a single degree of freedom forced vibration system. The stimulated vibration excitation depends on the acceleration of base vibration and the magnitude of the equivalent base force is $m\ddot{u}$. Fig. 3 shows the equivalence of translational base excitation.

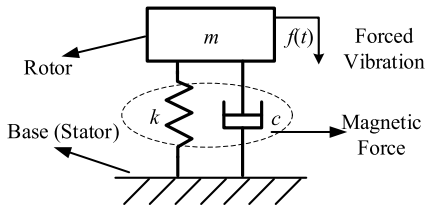

FIGURE 3. The equivalence of translational base excitation.

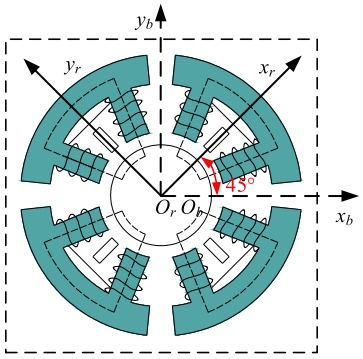

FIGURE 4. The magnetic poles in the test rig adopted in this paper are inclined 45 degrees to the horizontal plane.

To express the translational base excitation, the rotor coordinate system is defined as $O_r x_r y_r z_r$, which is fixed to the rotor and moving with the rotor. The base coordinate system is defined as $O_b x_b y_b z_b$. As shown in the Fig. 4, in order to improve the magnetic force load capacity, the magnetic poles in test rig adopted here are inclined 45 degrees to the horizontal plane. Therefore, the rotor translational equation of motion in both x and y directions can be expressed as

$$\begin{cases} m\ddot{x} = F_x + U_x \\ m\ddot{y} = F_y + U_y \end{cases} \tag{4}$$

where F is the other generalized forces except base, U_x and U_y are the equivalent base forces in x and y direction,

$$\begin{cases} U_x = -\sqrt{2}/2m(\ddot{u}_x - \ddot{u}_y) \\ U_y = -\sqrt{2}/2m(\ddot{u}_x + \ddot{u}_y) \end{cases} \tag{5}$$

Eq. (4-5) indicate that the translational base motion applied to the system can be equivalent to the external force applied to the rotor.

B. MODELING THE ROTATIONAL BASE MOTION

For the rotor (Fig. 5), the z direction is the rotational axis, therefore, it is only necessary to study the rotational base

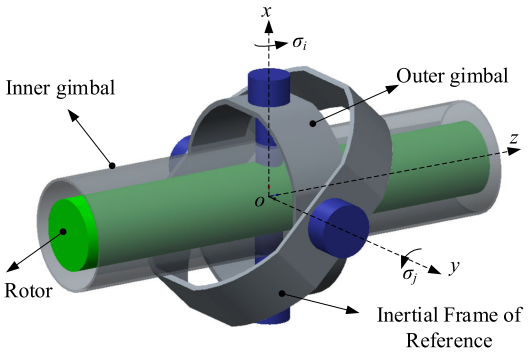

FIGURE 5. The coordinates of rotor double-gimbal system.

motion in x and y direction. When the translational base motion is not considered, the rotational base motion system comprised of the rotor and the base can be regarded as a double-gimbal system [8], [28], as shown in Fig. 5.

The rotation of the base in the x and y directions can be equivalent to the superposition of the two gimbals rotation. Before the derivation of rotational motion, the reference coordinate systems and transformation matrixes need to be established firstly. As shown in Fig. 5, $O_j x_j y_j z_j$ is the outer gimbal coordinate system, $O_g x_g y_g z_g$ is the inner gimbal coordinate system, $O_i x_i y_i z_i$ represents the inertial coordinate system.

The outer gimbal coordinate system $O_j x_j y_j z_j$ coincides with the inertial coordinate system $O_i x_i y_i z_i$ under initial conditions and has only rotational freedom about the inertial frame y_i axis. The rotational angle and angular velocity of the outer gimbal are denoted as θ_j. and σ_j. Therefore, the transformation matrix between the outer gimbal coordinate system and the inertial coordinate system $O_i x_i y_i z_i$ is

$$\begin{bmatrix} x_j \\ y_j \\ z_j \end{bmatrix} = \begin{bmatrix} \cos\theta_j & 0 & -\sin\theta_j \\ 0 & 1 & 0 \\ \sin\theta_j & 0 & \cos\theta_j \end{bmatrix} \begin{bmatrix} x_i \\ y_i \\ z_i \end{bmatrix} = C_i^j \begin{bmatrix} x_i \\ y_i \\ z_i \end{bmatrix} \tag{6}$$

The inner gimbal coordinate system $O_g x_g y_g z_g$ coincides with the inertial coordinate system under initial conditions and has only rotational freedom about the outer gimbal x_g axis. The rotation angle and angular velocity of the inner gimbal are denoted as θ_i. and σ_i. Therefore, the transformation matrix between the inner gimbal coordinate system and the outer gimbal coordinate system is

$$\begin{bmatrix} x_g \\ y_g \\ z_g \end{bmatrix} = \begin{bmatrix} 1 & 0 & 0 \\ 0 & \cos\theta_i & \sin\theta_i \\ 0 & -\sin\theta_i & \cos\theta_i \end{bmatrix} \begin{bmatrix} x_j \\ y_j \\ z_j \end{bmatrix} = C_j^g \begin{bmatrix} x_j \\ y_j \\ z_j \end{bmatrix} \tag{7}$$

The rotor base coordinate system $O_b x_b y_b z_b$ is fixed to the inner gimbal coordinate system with 45 degrees inclination to the horizontal plane (Fig.4). Therefore, the transformation matrix between the base coordinate system and the inner gimbal coordinate system is

$$\begin{bmatrix} x_b \\ y_b \\ z_b \end{bmatrix} = \begin{bmatrix} \sqrt{2}/2 & -\sqrt{2}/2 & 0 \\ \sqrt{2}/2 & \sqrt{2}/2 & 0 \\ 0 & 0 & 1 \end{bmatrix} \begin{bmatrix} x_g \\ y_g \\ z_g \end{bmatrix} = C_g^b \begin{bmatrix} x_g \\ y_g \\ z_g \end{bmatrix} \tag{8}$$

To establish the rotor rotation dynamics equation, a standard reference coordinate system is needed for transforming other coordinate systems to this standard system. The standard coordinate system, defined as $O_r x_f y_f z_f$ and named as inner ring coordinate system, presents the coordinate system wherein the rotor inclines at an angle (α, β) relative to the base. The inner ring and the rotor coordinate systems can separate the relative angular from spin motion of the rotor. The rotor coordinate system $O_r x_r y_r z_r$ describes the spin of the rotor and the inner ring coordinate system $O_r x_f y_f z_f$ illustrates the angular motion of the rotor. Under initial conditions, the inner ring system coincides with the base coordinate system. Therefore, the transformation matrix between the inner ring coordinate system and the base coordinate system is

$$\begin{aligned}\begin{bmatrix} x_f \\ y_f \\ z_f \end{bmatrix} &= \begin{bmatrix} \cos\beta & 0 & -\sin\beta \\ \sin\alpha\sin\beta & \cos\alpha & \sin\alpha\sin\beta \\ \cos\alpha\sin\beta & -\sin\alpha & \cos\alpha\sin\beta \end{bmatrix} \begin{bmatrix} x_b \\ y_b \\ z_b \end{bmatrix} \\ &= C_b^f \begin{bmatrix} x_b \\ y_b \\ z_b \end{bmatrix} \end{aligned} \tag{9}$$

In the rotor coordinate system $O_r x_r y_r z_r$, due to the rotor spin around the z_r axis, the transformation matrix between the rotor coordinate system and the inner ring coordinate system is

$$\begin{bmatrix} x_r \\ y_r \\ z_r \end{bmatrix} = \begin{bmatrix} \cos\Omega t & \sin\Omega t & 0 \\ -\sin\Omega t & \cos\Omega t & 0 \\ 0 & 0 & 1 \end{bmatrix} \begin{bmatrix} x_f \\ y_f \\ z_f \end{bmatrix} = C_f^r \begin{bmatrix} x_f \\ y_f \\ z_f \end{bmatrix} \tag{10}$$

where Ω is the rotor spin speed.

The rotor absolute rotational motion includes three parts, (1) the rotor rotates relatively to the base, which is described using α, β, Ω; (2) the base rotates relatively to the outer gimbal, which is described using θ_i.; (3) the outer gimbal rotates relatively to the inertial frame, which is described using θ_j. For the rotational base motion, since only the x and y direction are considered, the equation of motion can be established in the inner ring coordinate system.

The rotor angular velocity ω_{br} relative to the base system is,

$$\omega_{br} = \omega_{bf} + \omega_{fr} = \dot{\alpha} + \dot{\beta} + \Omega \tag{11}$$

whose projection in the inner ring system can be written as

$$\omega_{br}^f = \omega_{bf}^f + \omega_{fr}^f \tag{12}$$

where

$$\begin{aligned}\omega_{bf}^f &= \begin{bmatrix} \dot{\alpha} \\ 0 \\ 0 \end{bmatrix} + \begin{bmatrix} 1 & 0 & 0 \\ 0 & \cos\alpha & \sin\alpha \\ 0 & -\sin\alpha & \cos\alpha \end{bmatrix} \begin{bmatrix} 0 \\ \dot{\beta} \\ 0 \end{bmatrix} \\ &= \begin{bmatrix} \dot{\alpha} \\ \dot{\beta}\cos\alpha \\ -\dot{\beta}\sin\alpha \end{bmatrix} \end{aligned} \tag{13}$$

and

$$\omega_{fr}^f = \begin{bmatrix} 0 \\ 0 \\ \Omega \end{bmatrix} \tag{14}$$

The inner gimbal angular velocity ω_{ig} relative to the inertial coordinate system is,

$$\omega_{ig} = \sigma_i + \sigma_j \tag{15}$$

whose projection in the inner ring system can be written as

$$\omega_{ig}^f = C_b^f C_g^b \omega_{ig}^g \tag{16}$$

where

$$\begin{aligned}\omega_{ig}^g &= \begin{bmatrix} \sigma_i \\ 0 \\ 0 \end{bmatrix} + \begin{bmatrix} 1 & 0 & 0 \\ 0 & \cos\theta_i & \sin\theta_i \\ 0 & -\sin\theta_i & \cos\theta_i \end{bmatrix} \begin{bmatrix} 0 \\ \sigma_j \\ 0 \end{bmatrix} \\ &= \begin{bmatrix} \sigma_i \\ \sigma_j\cos\theta_i \\ -\sigma_j\sin\theta_i \end{bmatrix} \end{aligned} \tag{17}$$

Therefore, combing Eq. (12) and Eq. (16), the projection of the rotor absolutely angular velocity in the inner gimbal coordinate system is

$$\begin{aligned}\omega_{ir}^f &= \omega_{br}^f + \omega_{ig}^f \\ &= \omega_{bf}^f + \omega_{fr}^f + C_b^f C_g^b \omega_{ig}^g \\ &= \begin{bmatrix} \dot{\alpha} \\ \dot{\beta}\cos\alpha \\ \Omega - \dot{\beta}\sin\alpha \end{bmatrix} \\ &\quad + \begin{bmatrix} \cos\beta & 0 & -\sin\beta \\ \sin\alpha\sin\beta & \cos\alpha & \sin\alpha\sin\beta \\ \cos\alpha\sin\beta & -\sin\alpha & \cos\alpha\sin\beta \end{bmatrix} \\ &\quad \times \begin{bmatrix} \sqrt{2}/2 & -\sqrt{2}/2 & 0 \\ \sqrt{2}/2 & \sqrt{2}/2 & 0 \\ 0 & 0 & 1 \end{bmatrix} \begin{bmatrix} \sigma_i \\ \sigma_j\cos\theta_i \\ -\sigma_j\sin\theta_i \end{bmatrix} \end{aligned} \tag{18}$$

For the rotor AMB system, given that rotor is restricted in the narrow air gap between the rotor and the touch-down bearing, the rotor rotational angle (α, β) is closed to zero. To simplify the following derivation, the base rotational angle (θ_i, θ_j) is assumed to be very small, therefore,

$$\begin{cases} \cos\alpha = \cos\beta = \cos\theta_i = \cos\theta_j \approx 1 \\ \sin\alpha = \sin\beta = \sin\theta_i = \cos\theta_j \approx 0 \end{cases} \tag{19}$$

Substitute Eq. (19) into Eq. (18) and obtain

$$\omega_{ir}^f = \begin{bmatrix} \dot{\alpha} + \sqrt{2}/2(\sigma_i - \sigma_j) \\ \dot{\beta} + \sqrt{2}/2(\sigma_i + \sigma_j) \\ \Omega \end{bmatrix} \tag{20}$$

The moment of inertia component for the rotor is denoted as,

$$J = \begin{bmatrix} J_r & 0 & 0 \\ 0 & J_r & 0 \\ 0 & 0 & J_z \end{bmatrix} \tag{21}$$

Therefore, the rotor angular momentum $H = \omega_{ir}^{f} \cdot J$ is

$$\begin{cases} H_x = J_r\left[\dot{\alpha} + \sqrt{2}/2(\sigma_i - \sigma_j)\right] \\ H_y = J_r\left[\dot{\beta} + \sqrt{2}/2(\sigma_i + \sigma_j)\right] \\ H_z = J_z\Omega \end{cases} \tag{22}$$

and the first order differential of Eq. (22) is

$$\begin{cases} dH_x/dt = J_r\left[\ddot{\alpha} + \sqrt{2}/2(\dot{\sigma}_i - \dot{\sigma}_j)\right] \\ dH_y/dt = J_r\left[\ddot{\beta} + \sqrt{2}/2(\dot{\sigma}_i + \dot{\sigma}_j)\right] \\ dH_z/dt = J_z\dot{\Omega} \end{cases} \tag{23}$$

For the rotor AMB system, there is no external torque in the axial direction according to the Euler equation. The external torque in the radial direction of the rotor is determined by the electromagnetic force and its distance from the center of mass. Therefore, the external torque M received by the rotor and the angular velocity ω of the inner ring system rotor can be written as

$$M = \begin{bmatrix} p_x \\ p_y \\ 0 \end{bmatrix} \tag{24}$$

and

$$\omega = \begin{bmatrix} \dot{\alpha} + \sqrt{2}/2(\sigma_i - \sigma_j) \\ \dot{\beta} + \sqrt{2}/2(\sigma_i + \sigma_j) \\ 0 \end{bmatrix} \tag{25}$$

The expression of Euler equation is

$$\begin{cases} \dot{H}_x + H_z\omega_y - H_y\omega_z = M_x \\ \dot{H}_y + H_x\omega_z - H_z\omega_x = M_y \\ \dot{H}_z + H_y\omega_x - H_x\omega_y = M_z \end{cases} \tag{26}$$

Substituting Eq. (22-25) into Eq. (26) yields

$$\begin{cases} J_r\ddot{\alpha} + J_z\Omega\dot{\beta} = p_x + Q_x \\ J_r\ddot{\beta} - J_z\Omega\dot{\alpha} = p_y + Q_y \end{cases} \tag{27}$$

where

$$\begin{cases} Q_x = -\sqrt{2}/2\left[(\dot{\sigma}_i - \dot{\sigma}_j) + J_z\Omega(\sigma_i + \sigma_j)\right] \\ Q_y = -\sqrt{2}/2\left[(\dot{\sigma}_i + \dot{\sigma}_j) - J_z\Omega(\sigma_i - \sigma_j)\right] \end{cases} \tag{28}$$

Eq. (27-28) indicates that the rotational base motion can be equivalent to the external torque applied to the rotor.

C. MODELING THE ROTOR UNBALANCE

Vibrations induced by mass unbalance is inevitable. The unbalance can be divided into static and dynamic unbalance. Assuming that the position of the unbalanced mass point is q_g and rotor centroid position is $q_c = [x, y, \alpha, \beta]$, the mass unbalance component can then be denoted as,

$$\Delta q = q_g - q_c = \begin{bmatrix} e\cos(\Omega t + \varphi) \\ e\sin(\Omega t + \varphi) \\ \varepsilon\cos(\Omega t + \gamma) \\ \varepsilon\sin(\Omega t + \gamma) \end{bmatrix} \tag{29}$$

where e and φ are the amplitude and phase of static unbalance, respectively, ε and γ are the amplitude and phase of dynamic unbalance, respectively. Therefore, the unbalance force can be written as

$$\begin{aligned} F_u &= \begin{bmatrix} F_{ux} \\ F_{uy} \\ M_{u\alpha} \\ M_{u\beta} \end{bmatrix} \\ &= \begin{bmatrix} me\Omega^2\cos(\Omega t + \varphi) \\ me\Omega^2\cos(\Omega t + \varphi) \\ J_r\varepsilon\Omega^2\cos(\Omega t + \gamma) + J_z\varepsilon\Omega^2\sin(\Omega t + \gamma) \\ J_r\varepsilon\Omega^2\sin(\Omega t + \gamma) + J_z\varepsilon\Omega^2\cos(\Omega t + \gamma) \end{bmatrix} \end{aligned} \tag{30}$$

For the rotor adopted in this AMB system, the length of the rotor is much larger than the radial size, therefore J_z can be negligible and Eq. (30) can be simplified as,

$$F_u = \begin{bmatrix} F_{ux} \\ F_{uy} \\ M_{u\alpha} \\ M_{u\beta} \end{bmatrix} = \begin{bmatrix} me\Omega^2\cos(\Omega t + \varphi) \\ me\Omega^2\cos(\Omega t + \varphi) \\ J_r\varepsilon\Omega^2\cos(\Omega t + \gamma) \\ J_r\varepsilon\Omega^2\sin(\Omega t + \gamma) \end{bmatrix} \tag{31}$$

D. EQUATION OF MOTION OF THE ROTOR CONSIDERING BASE MOTION

Combing the above derivation, the equation of motion of the rotor considering base motion is

$$\begin{cases} m\ddot{x} = f_{x1} + f_{x2} + U_x + F_{ux} \\ m\ddot{y} = f_{y1} + f_{y2} + U_y + F_{uy} \\ J_r\ddot{\alpha} + J_z\Omega\dot{\beta} = l_1 f_{y1} - l_2 f_{y2} + Q_x + M_{ua} \\ J_r\ddot{\beta} - J_z\Omega\dot{\alpha} = -l_1 f_{y1} + l_2 f_{y2} + Q_y + M_{u\beta} \end{cases} \tag{32}$$

and the matrix expression of Eq. (32) can be expressed as

$$M\ddot{q}_c + G\dot{q}_c = F_u + F_b + Bf \tag{33}$$

where f is magnetic force provided by the AMB, M is the mass matrix, G is the gyroscopic matrix, F_b is the equivalent generalized force matrix generated by basic vibration, B is the matrix relevant to magnet force. These vectors and matrixes can be written as,

$$f = \begin{bmatrix} f_{x1} & f_{y2} & f_{x2} & f_{y2} \end{bmatrix}^T \tag{34}$$

$$M = \begin{bmatrix} m & 0 & 0 & 0 \\ 0 & m & 0 & 0 \\ 0 & 0 & J_r & 0 \\ 0 & 0 & 0 & J_r \end{bmatrix} \tag{35}$$

$$G = \begin{bmatrix} 0 & 0 & 0 & 0 \\ 0 & 0 & 0 & 0 \\ 0 & 0 & 0 & J_z\Omega \\ 0 & 0 & -J_z\Omega & 0 \end{bmatrix} \tag{36}$$

$$B = \begin{bmatrix} 1 & 0 & 1 & 0 \\ 0 & 1 & 0 & 1 \\ 0 & l_1 & 0 & -l_2 \\ -l_1 & 0 & l_2 & 0 \end{bmatrix} \tag{37}$$

$$F_b = \begin{bmatrix} U_x & U_y & Q_x & Q_y \end{bmatrix}^T \tag{38}$$

In the rotor AMB system, the data obtained from the displacement sensor is adopted for calculation. However, as shown in Fig. 6, due to the sensor and actuator non-collocation, the transform relation between the centroid displacement q_c, the actuator displacement q_d and the sensor results q_h should be established firstly. Table 2 lists the parameters of the rotor.

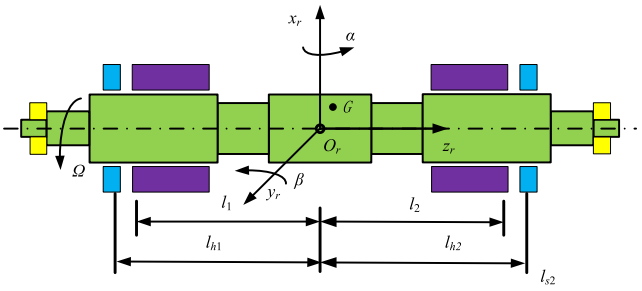

FIGURE 6. The sensor and actuator non-collocation view.

TABLE 2. Parameters for the rotor.

Symbol	Parameter	Values
m	Rotor mass	2.4 kg
J_r	Moment of inertia	1.612×10^{-2} kg·m^2
J_z	Polar moment of inertia	3.8×10^{-4} kg·m^2
l_1	Distance between left AMB and center of mass	116 mm
l_2	Distance between right AMB and center of mass	116 mm
l_{h1}	Distance between left sensor and center of mass	101 mm
l_{h2}	Distance between right sensor and center of mass	89 mm
l_{s1}	Distance between left touch-down bearing and center of mass	161 mm
l_{s2}	Distance between right touch-down bearing and center of mass	167 mm

The displacement of the actuator is denoted as

$$q_d = \begin{bmatrix} x_1 & y_1 & x_2 & y_2 \end{bmatrix}^T \tag{39}$$

and the displacement of the sensor is denoted as

$$q_h = \begin{bmatrix} x_{h1} & y_{h1} & x_{h2} & y_{h2} \end{bmatrix}^T \tag{40}$$

The transformation matrix for the centroid displacement q_c is

$$\begin{cases} q_c = Rq_d \\ q_c = Hq_h \end{cases} \tag{41}$$

where

$$R = \frac{1}{l_1 + l_2} \begin{pmatrix} l_2 & 0 & l_1 & 0 \\ 0 & l_2 & 0 & l_1 \\ 0 & 1 & 0 & -1 \\ -1 & 0 & 1 & 0 \end{pmatrix} \tag{42}$$

and

$$H = \frac{1}{l_{h1} + l_{h2}} \begin{pmatrix} l_{h2} & 0 & l_{h1} & 0 \\ 0 & l_{h2} & 0 & l_{h1} \\ 0 & 1 & 0 & -1 \\ -1 & 0 & 1 & 0 \end{pmatrix} \tag{43}$$

The magnetic force provide by the AMBs could be modeled as stiffness and damping force,

$$f = -Kq_d - C\dot{q}_d \tag{44}$$

where $K = diag[k_{x1}k_{y1}\ k_{x2}k_{y2}]$ is the equivalent stiffness, $C = diag[c_{x1}c_{y1}\ c_{x2}c_{y2}]$ is the equivalent damping [29]. Substitute Eq. (41-44) into Eq. (33) and obtained,

$$MH\ddot{q}_h + \left(G + BCR^{-1}\right) H\dot{q}_h + BKR^{-1}Hq_h = F_u + F_b \tag{45}$$

Eq. (45) is the AMB system dynamic model considering the base motion.

In order to perform the subsequent dynamic analysis, we consider the influence of the impact base motion on the rotor displacement amplitude. Given that the base impact is more likely to induce rotor instability, the rotor would touch the touch bearings. Thus, the displacement of the rotor at touch-down bearing q_s is selected to establish the dynamic equation. The equation is similar to the displacement at the sensor, the derivation is as follows,

$$q_c = Tq_s \tag{46}$$

where

$$T = \frac{1}{l_{s1} + l_{s2}} \begin{pmatrix} l_{s2} & 0 & l_{s1} & 0 \\ 0 & l_{s2} & 0 & l_{s1} \\ 0 & 1 & 0 & -1 \\ -1 & 0 & 1 & 0 \end{pmatrix} \tag{47}$$

$$MT\ddot{q}_s + \left(G + BCR^{-1}\right) T\dot{q}_s + BKR^{-1}Tq_s = F_u + F_b \tag{48}$$

IV. THE EFFECT OF IMPACT BASE MOTION FOR AMB SYSTEM

From the time domain, the base motion could be classified into continuous excitation and short-time impact excitation. The impact base motion may cause serious damage to AMB system since the momentum is changing in a very short time. Therefore, we adopt the impact base motion in the following dynamic analysis. The displacement data x_{s1} for AMB1 at touch-down bearing position in x direction is selected for analysis.

A. COMPARISON OF TRANSLATIONAL AND ROTATIONAL IMPACT FOR AMB SYSTEM

For the translational base motion, semi-sinusoidal and rectangular impact excitation forms are adopted. In the case of rotational base motion, sinusoidal impact excitation form is adopted. The translational excitation applied to the translational freedom degree equation of rotor acts as force and the rotational excitation applied to the rotational

freedom degree equation of rotor plays the role of torque. The differential Eq. (48) is evaluated numerically using the fourth-order Runge–Kutta algorithm with 0.001s step and the transient response is obtained. Table 3 lists the parameters for impact base motion simulation. The time domain displacement response is analyzed between 0 and 2s and the impact excitation is applied at 1s.

TABLE 3. Parameters for the impact base motion simulation.

Symbol	Quantity	Values
k	*AMB stiffness*	10^6 N/m
c	*AMB damping*	700 N·s/s
z_1	translational excitation amplitude	10 g
z_2	translational excitation width	20 ms
M_{s1}	rotational excitation amplitude	100 π
M_{s2}	rotational excitation frequency	50 Hz
e	eccentricity	5 μm

The displacement x_{s1} obtained under translational excitation is illustrated in Fig. 7. The blue line represents the semi-sinusoidal impact excitation response and the red line is the rectangular impact excitation response. It can be seen that the application of base motion can significantly stimulate the increase of displacement. The maximum amplitudes corresponding to semi-sinusoidal and rectangular excitation are 0.09mm and 0.11mm, respectively.

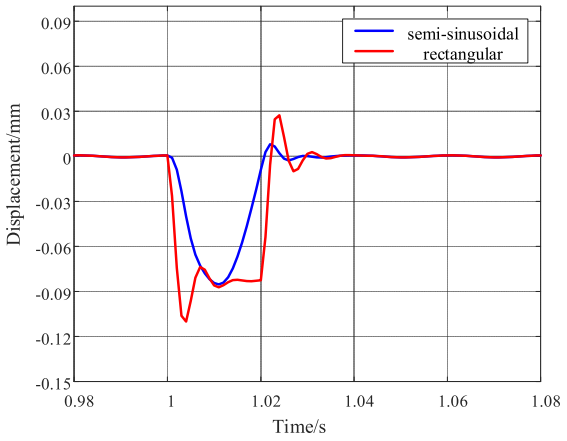

FIGURE 7. The rotor responses at x_{s1} only the translational excitation is applied.

Shown in Fig. 8 are the displacement x_{s1} upon the application of semi-sinusoidal translational with/without rotational excitation. It is found that the rotational excitation has small effect on the amplitude of displacement. However, on the other hand, the rotational excitation can yield a phase lag. Fig. 9 compares the displacement x_{s1} upon the application of rectangular translational with/without rotational excitation. Clearly, one can see that the resultant displacement is mainly dependent on rectangular translational excitation. The rotational base motion appears to slightly enhance the amplitude of displacement.

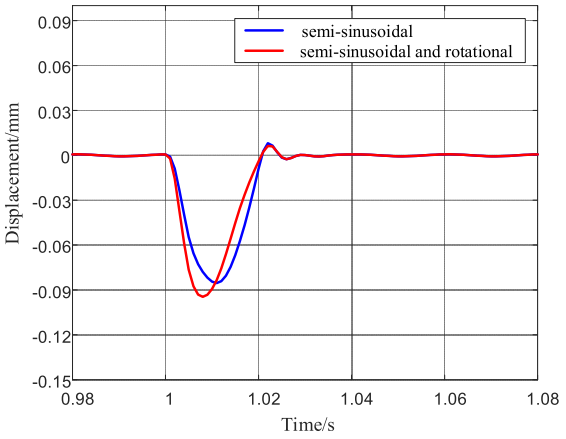

FIGURE 8. Comparison of semi-sinusoidal translational and rotational Impact base motion for AMB System.

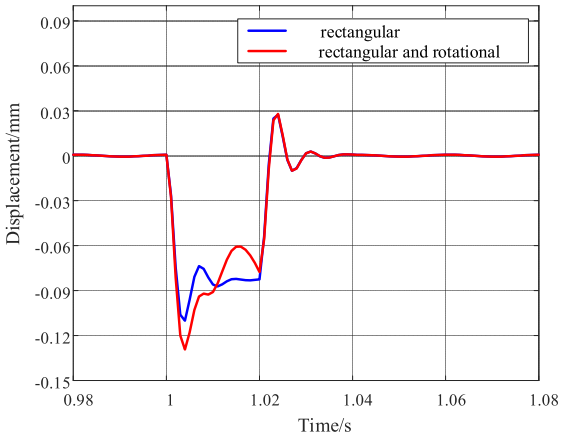

FIGURE 9. Comparison of rectangular translational and rotational Impact base motion for AMB System.

B. EFFECT OF IMPACT AMPLITUDE AND WIDTH

A systematic investigation regarding the effect of amplitude and width corresponding to translational and rotational impact base motion on displacement x_{s1} is performed here. As the first step, we analyze the influence of amplitude and width corresponding to translational impact base motion on displacement x_{s1}.

Presented in Fig. 10 are the displacement x_{s1} versus amplitude and width upon the semi-sinusoidal translational excitation. Here, the translational amplitude increases from 1g to 12g by 1g and the width increases from 2ms to 40ms by 2ms. Other parameters such as AMB stiffness and damping which listed in table 3 remain unchanged. From Fig.10, it can be concluded that rotor displacement increases linearly in proportion to the impact amplitude. Meanwhile, the width fluctuation seems to have negligible effect on the rotor displacement, particularly in the cases wherein the width is over 8ms.

Fig. 11 gives the displacement x_{s1} versus amplitude and width upon the rectangular translational excitation. Similar to the changing-trend mentioned above, the rotor displacement

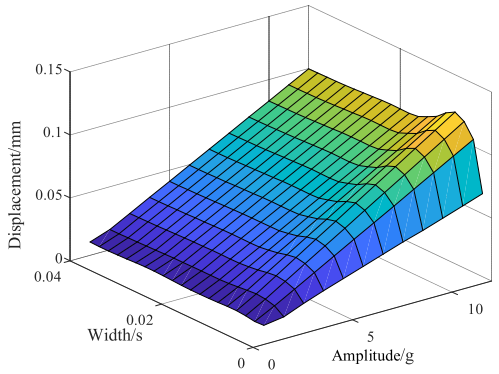

FIGURE 10. The displacement versus impact amplitude and width of semi-sinusoidal translational base motion.

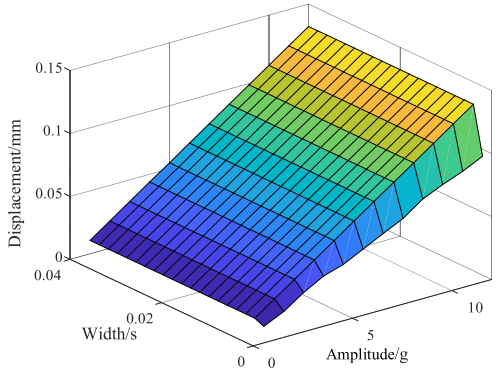

FIGURE 11. The displacement versus impact amplitude and width of rectangular translational base motion.

appears to remain almost unchanged with increasing width and raise linearly in proportion to the impact amplitude.

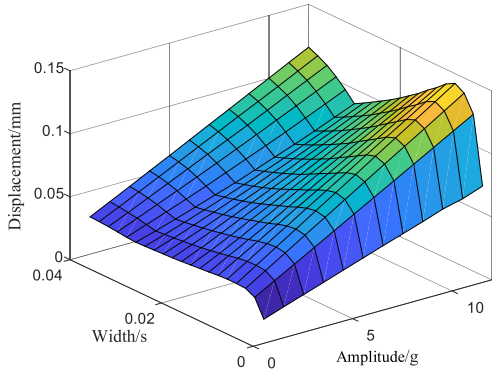

FIGURE 12. The displacement versus impact amplitude and width considering both semi-sinusoidal translational and rotational base motion.

The displacement x_{s1} versus amplitude and width upon the semi-sinusoidal translational excitation and rotational excitation are manifested in Fig. 12. Apparently, with the increase of amplitude, a sudden collapse in displacement occurs in the width range of 20-40ms. This may be attributed to the fact that the rotational and translational excitation cancel out in the opposite phase. The collapse position is related to the pulse width of the excitation.

Accordingly, displacement x_{s1} versus amplitude and width upon the rectangular translational excitation and rotational

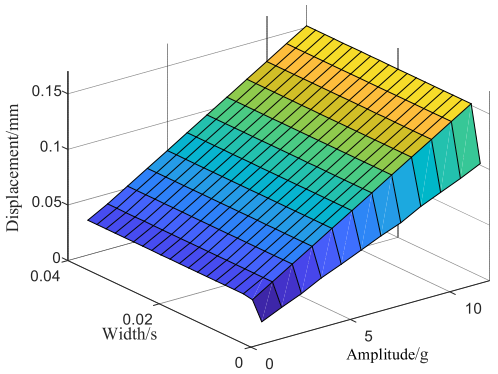

FIGURE 13. The displacement versus impact amplitude and width considering both rectangular translational and rotational base motion.

excitation are illustrated in Fig. 13. Interestingly, the changing trends of x_{s1} versus amplitude and width is similar to these found in Fig.11 wherein only rectangular translational excitation is applied. Thus, it is deduced that the rotational excitation has little effect on the rotor displacement responses.

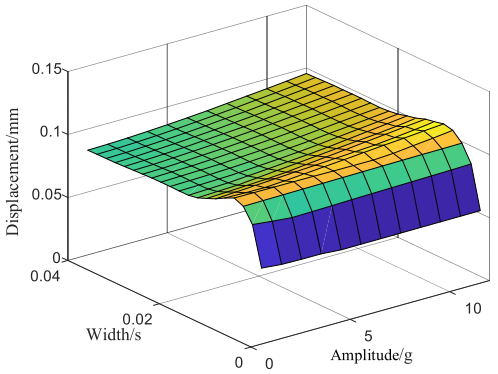

FIGURE 14. The displacement versus impact amplitude and width of rotational base motion with semi-sinusoidal translational motion.

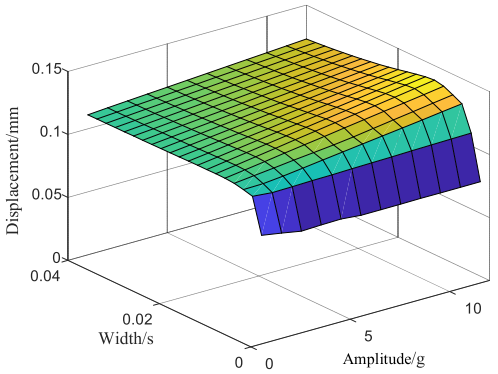

FIGURE 15. The displacement versus impact amplitude and width of rotational base motion with rectangular translational motion.

In the second step, the influence of amplitude and width corresponding to rotational impact base motion on displacement x_{s1} is discussed. Shown in Fig. 14 and Fig. 15 are the displacement x_{s1} versus amplitude and width upon the

rotational impact base motion with semi-sinusoidal translational excitation and rectangular translational excitation, respectively. The rotational excitation amplitude increases from 1 π to 120 π and the width increases from 0ms to 40ms. Other parameters such as AMB stiffness and damping which listed in table 3 remain unchanged. From Fig.14 and Fig.15, it can be concluded that the rotational impact amplitude and width have rather small effect on the rotor responses.

C. EFFECT OF EQUIVALENT STIFFNESS AND DAMPING

For the AMB system, the electromagnetic force parameters, equivalent stiffness and damping are critical factors for the rotor dynamics analysis. In this work, the effect of stiffness and damping on displacement x_{s1} upon the base motion is explored.

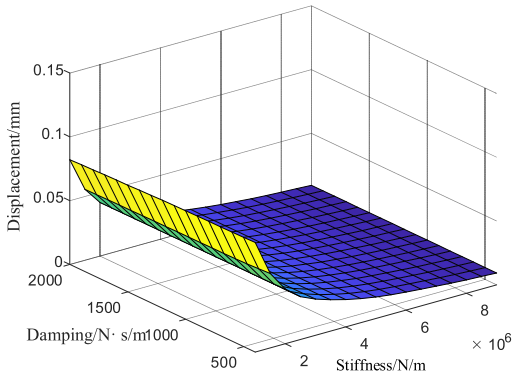

FIGURE 16. The displacement versus stiffness and damping upon semi-sinusoidal translational motion.

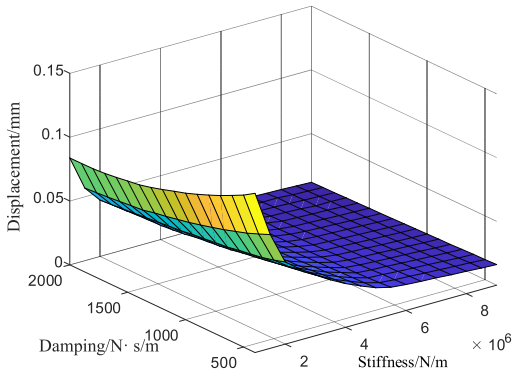

FIGURE 17. The displacement versus stiffness and damping upon rectangular translational motion.

Fig. 16 and Fig. 17 display the obtained displacement x_{s1} versus stiffness and damping upon semi-sinusoidal and rectangular translational excitation, respectively. The stiffness increases from 1×10^6 N/m to 9×10^6 N/m by 0.5×10^6 N/m and the damping increases from 400 N·s/m to 2000 N·s/m by 100 N·s/m. Other parameters which are plotted in table 3 remain unchanged. As can be seen in Fig.16 and Fig.17, the displacement performs a consistently decline with the increasing of the equivalent stiffness. When the stiffness is of relatively low level, the displacements upon semi-sinusoidal and rectangular translational excitation are almost comparable. It also should be noted there that, compared with the equivalent stiffness, the equivalent damping has much weaker effect on the displacement, particularly in the cases wherein rectangular translational excitation is applied.

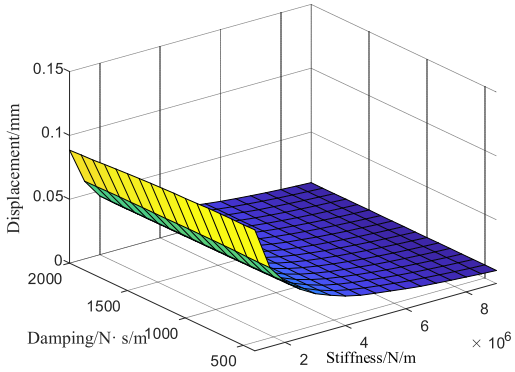

FIGURE 18. The displacement versus stiffness and damping upon semi-sinusoidal translational and rotational motion.

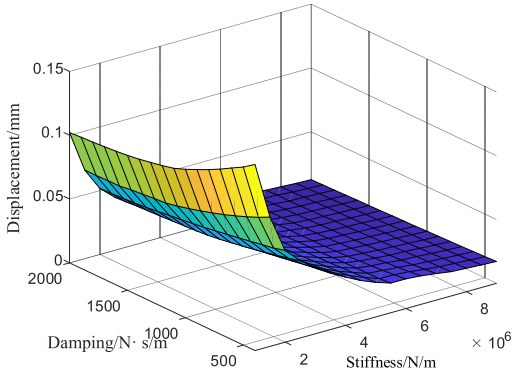

FIGURE 19. The displacement versus stiffness and damping upon rectangular translational and rotational motion.

The effect of stiffness and damping on displacement upon the combination of translational and rotational base motion is also evaluated here. Fig.18 and 19 show the displacement x_{s1} versus stiffness and damping upon rotational base motion with semi-sinusoidal and rectangular translational excitation, respectively. Clearly, upon the combination of translational and rotational base motion, the amplitude of displacement can be strengthened as compared with those upon simply translational base motion. However, the changing trends of displacements with increasing stiffness and damping are similar to those observed in cases wherein only translational excitations are applied.

V. CONCLUSION

In this work, a dynamic modeling method for AMB system operating in base motion condition is developed and presented wherein both translational and rotational base motions are both considered. The derivation indicates that the translational base motion is equivalent to the external force applied to the rotor and the rotational base motion is equivalent to the external torque applied to the rotor. Then, considering the influence of rotor unbalance mass and equivalent electromagnetic force, the dynamic equation of

AMB system operating in base motion condition is established. Furthermore, making use of the proposed dynamic model, we analyze the dynamics of rotor displacement in the impact base motion condition from the aspects of excitation amplitude, pulse width and supporting parameters.

The results reveal the predominant role of translational excitation, particularly the rectangular translational excitation in affecting the performance of AMB system. The rotation excitation can only slightly enhance the overall displacement amplitude. Upon the application of individual translational excitation, the rotor displacement amplitude shows a linear correlation with the impact amplitude while it is rarely affected by the pulse width of excitation. In the case wherein individual rotational excitation is applied, neither impact amplitude nor pulse width of excitation has obvious effect on the rotor displacement amplitude. However, the coupling effect of translational and rotational excitations on rotor displacement amplitude cannot be ignored. Moreover, it can be concluded that the support stiffness is the main factor to restrain the rotor displacement, and the support damping has little effect on the rotor displacement amplitude.

REFERENCES

[1] G. Schweitzer and E. H. Maslen, *Magnetic Bearings: Theory, Design, and Application to Rotating Machinery*. Berlin, Germany: Springer, 2009.

[2] A. H. Pesch, A. Smirnov, O. Pyrhonen, and J. T. Sawicki, "Magnetic bearing spindle tool tracking through μ-synthesis robust control," *IEEE/ASME Trans. Mechatronics*, vol. 20, no. 3, pp. 1448–1457, Jun. 2015, doi: 10.1109/TMECH.2014.2344592.

[3] S. Zheng, B. Han, Y. Wang, and J. Zhou, "Optimization of damping compensation for a flexible rotor system with active magnetic bearing considering gyroscopic effect," *IEEE/ASME Trans. Mechatronics*, vol. 20, no. 3, pp. 1130–1137, Jun. 2015, doi: 10.1109/TMECH.2014.2344664.

[4] S. Y. Yoon, Z. Lin, K. T. Lim, C. Goyne, and P. E. Allaire, "Model validation for an active magnetic bearing based compressor surge control test rig," *J. Vib. Acoust.*, vol. 132, no. 6, p. 061005, Dec. 2010, doi: 10.1115/1.4001845.

[5] M. Sig Kang and W. Hyun Yoon, "Acceleration feedforward control in active magnetic bearing system subject to base motion by filtered-X LMS algorithm," *IEEE Trans. Control Syst. Technol.*, vol. 14, no. 1, pp. 134–140, Jan. 2006.

[6] M. A. Pichot, J. P. Kajs, B. R. Murphy, A. Ouroua, B. M. Rech, R. J. Hayes, J. H. Beno, G. D. Buckner, and A. B. Palazzolo, "Active magnetic bearings for energy storage systems for combat vehicles," *IEEE Trans. Magn.*, vol. 37, no. 1, pp. 318–323, Jan. 2001.

[7] J. Nelson, J. Watkins, and G. Piper, "Active control of fan noise in ducts using magnetic bearings," in *Proc. 8th AIAA/CEAS Aeroacoustics Conf. Exhib.*, Jun. 2002, p. 2500.

[8] I. Jikuya, K. Fujii, and K. Yamada, "Attitude maneuver of spacecraft with a variable-speed double-gimbal control moment gyro," *Adv. Space Res.*, vol. 58, no. 7, pp. 1303–1317, Oct. 2016.

[9] C. Knospe and E. G. Collins, "Introduction to the special issue on magnetic bearing control [Guest Editorial]," *IEEE Trans. Control Syst. Technol.*, vol. 4, no. 5, p. 481, Sep. 1996.

[10] Y. Yi, Z. Qiu, and Q. Han, "The effect of time-periodic base angular motions upon dynamic response of asymmetric rotor systems," *Adv. Mech. Eng.*, vol. 10, no. 3, Mar. 2018, Art. no. 168781401876717, doi: 10.1177/1687814018767172.

[11] Q. Han and F. Chu, "Parametric instability of flexible rotor-bearing system under time-periodic base angular motions," *Appl. Math. Model.*, vol. 39, no. 15, pp. 4511–4522, Aug. 2015, doi: 10.1016/j.apm.2014.10.064.

[12] L. Hou, H. Chen, Y. Chen, K. Lu, and Z. Liu, "Bifurcation and stability analysis of a nonlinear rotor system subjected to constant excitation and rub-impact," *Mech. Syst. Signal Process.*, vol. 125, pp. 65–78, Jun. 2019, doi: 10.1016/j.ymssp.2018.07.019.

[13] L. Hou, Y. Chen, Y. Fu, and Z. Li, "Nonlinear response and bifurcation analysis of a duffing type rotor model under sine maneuver load," *Int. J. Non-Linear Mech.*, vol. 78, pp. 133–141, Jan. 2016, doi: 10.1016/j.ijnonlinmec.2014.12.012.

[14] L. Chen, J. Wang, Q. Han, and F. Chu, "Nonlinear dynamic modeling of a simple flexible rotor system subjected to time-variable base motions," *J. Sound Vib.*, vol. 404, pp. 58–83, Sep. 2017, doi: 10.1016/j.jsv.2017.05.032.

[15] Z. Liu, Z. Liu, Y. Li, and G. Zhang, "Dynamics response of an on-board rotor supported on modified oil-film force considering base motion," *Proc. Inst. Mech. Eng., C, J. Mech. Eng. Sci.*, vol. 232, no. 2, pp. 245–259, Jan. 2018, doi: 10.1177/0954406216682052.

[16] M. E. Kasarda, J. Clements, A. L. Wicks, C. D. Hall, and R. G. Kirk, "Effect of sinusoidal base motion on a magnetic bearing," in *Proc. IEEE Int. Conf. Control Appl.*, Sep. 2000, pp. 144–149.

[17] M. O. T. Cole, P. S. Keogh, and C. R. Burrows, "Vibration control of a flexible rotor/magnetic bearing system subject to direct forcing and base motion disturbances," *Proc. Inst. Mech. Eng., C, J. Mech. Eng. Sci.*, vol. 212, no. 7, pp. 535–546, Jul. 1998.

[18] M. S. Kang, "Optimal feedforward control of active magnetic bearing system subject to base motion," in *Proc. IEEE Conf. Control Appl. (CCA)*, Jun. 2003, pp. 748–753.

[19] M. S. Kang, J. Lyou, and J. K. Lee, "Sliding mode control for an active magnetic bearing system subject to base motion," *Mechatronics*, vol. 20, no. 1, pp. 171–178, Feb. 2010.

[20] H.-S. Kim, H.-Y. Kim, C.-W. Lee, and T.-H. Kang, "Stabilization of active magnetic bearing system subject to base motion," in *Proc. 19th Biennial Conf. Mech. Vib. Noise, Parts A, B, C*, vol. 5, Jan. 2003, pp. 2007–2013.

[21] S. Marx and C. Nataraj, "Suppression of base excitation of rotors on magnetic bearings," *Int. J. Rotating Machinery*, vol. 2007, pp. 1–10, Mar. 2007.

[22] C. Zhu, "Effect of impact on the dynamics of a rotor supported on active magnetic bearings," in *Proc. 21st IMAC Conf. Expo. (IMAC XXI), Conf. Expo. Struct. Dyn. Desc, Meeting Held*, Kissimmee, FL, USA, Feb. 2003, pp. 1–7.

[23] W. W. Zhang, "Coupled dynamic analysis of magnetic bearing-rotor system under the influences of base motion," *Appl. Mech. Mater.*, vol. 109, pp. 199–203, Oct. 2011.

[24] T. Soni, J. K. Dutt, and A. S. Das, "Parametric stability analysis of active magnetic bearing supported rotor system with a novel control law subject to periodic base motion," *IEEE Trans. Ind. Electron.*, vol. 67, no. 2, pp. 1160–1170, Feb. 2020, doi: 10.1109/TIE.2019.2898604.

[25] H.-S. Han, "A study on the dynamic modeling of a magnetic levitation vehicle," *JSME Int. J. C*, vol. 46, no. 4, pp. 1497–1501, 2003, doi: 10.1299/jsmec.46.1497.

[26] Y. Sun, J. Xu, H. Qiang, and G. Lin, "Adaptive neural-fuzzy robust position control scheme for maglev train systems with experimental verification," *IEEE Trans. Ind. Electron.*, vol. 66, no. 11, pp. 8589–8599, Nov. 2019, doi: 10.1109/TIE.2019.2891409.

[27] Y. Sun, J. Xu, H. Qiang, C. Chen, and G. Lin, "Adaptive sliding mode control of maglev system based on RBF neural network minimum parameter learning method," *Measurement*, vol. 141, pp. 217–226, Jul. 2019, doi: 10.1016/j.measurement.2019.03.006.

[28] H. Li, S. Yang, and H. Ren, "Dynamic decoupling control of DGCMG gimbal system via state feedback linearization," *Mechatronics*, vol. 36, pp. 127–135, Jun. 2016.

[29] Y. Xu, J. Zhou, Z. Lin, and C. Jin, "Identification of dynamic parameters of active magnetic bearings in a flexible rotor system considering residual unbalances," *Mechatronics*, vol. 49, pp. 46–55, Feb. 2018.

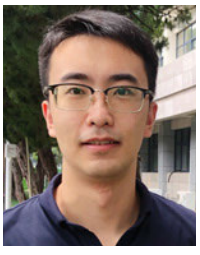

YUANPING XU (Member, IEEE) received the Ph.D. degree in mechanical engineering from the Nanjing University of Aeronautics and Astronautics (NUAA), in 2018. From 2016 to 2017, he was a Guest Ph.D. Student with the Ecole Polytechnique Federale Lausanne (EPFL), Switzerland. He is currently a Lecturer with the College of Mechanical and Electrical Engineering, NUAA. His research interests include high-performance magnetic levitation systems and manufacturing.

QUAN SHEN received the B.S. degree from the Hebei University of Engineering, in 2019. He is currently pursuing the M.S. degree with the Nanjing University of Aeronautics and Astronautics (NUAA). His research interest includes magnetic bearings.

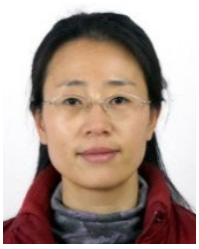

JIN ZHOU received the Ph.D. degree in mechanical engineering from the China University of Mining and Technology (CUMT), in 2001. From 2012 to 2013, she was a Visiting Scholar with the Rotating Machinery and Control Laboratory (ROMAC), University of Virginia. She is currently a Full Professor with the College of Mechanical and Electrical Engineering, Nanjing University of Aeronautics and Astronautics (NUAA). Her research interests include magnetic bearings and vibration control. She was the member of Program Committee of the 14th International Symposium on Magnetic Bearings (ISMB, 2014) and the Program Chair of the 16th International Symposium on Magnetic Bearings (ISMB, 2018). She was an Elected Member of the International Advisory Committee of ISMB, in 2018.

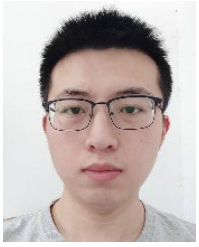

YUE ZHANG received the B.S. degree from the Nanjing University of Aeronautics and Astronautics (NUAA), in 2018, where he is currently pursuing the Ph.D. degree in mechanical design and theory. His research interest includes magnetic bearings.

CHAOWU JIN received the B.S., M.S., and Ph.D. degrees in mechanical engineering from the Nanjing University of Aeronautics and Astronautics (NUAA). He is currently an Associate Professor with the College of Mechanical and Electrical Engineering, NUAA. His research interest includes magnetic bearings.